

Supplementary Information

For

Diverse mechanisms of translation arrest by a Clostridia ribosome stalling peptide CliM

Mayu Yoshida^{1,*}, Felix Gersteuer^{2,*}, Ole Berendes³, Keigo Fujiwara^{1,4}, Haaris A. Safdari², Helge Paternoga², Hiraku Takada^{1,5}, Nozomu Obana^{6,7}, Helmut Grubmüller³, Lars Bock³, Daniel N. Wilson^{2,#}, Shinobu Chiba^{1,#}

¹ Faculty of Life Sciences and Institute for Protein Dynamics, Kyoto Sangyo University, Kamigamo, Motoyama, Kita-ku, Kyoto 603-8555, Japan.

² Institute for Biochemistry and Molecular Biology, Martin-Luther-King-Platz 6, University of Hamburg, 20146 Hamburg, Germany.

³ Department of Theoretical and Computational Biophysics, Max Planck Institute for Multidisciplinary Sciences, Göttingen, Germany

⁴ Department of Gene Function and Phenomics, National Institute of Genetics, Mishima, Japan

⁵ Biotechnology Research Center and Department of Biotechnology, Toyama Prefectural University, 5180 Kurokawa, Imizu, Toyama 939-0398, Japan

⁶ Transborder Medical Research Center, Institute of Medicine, University of Tsukuba, Tsukuba, Japan

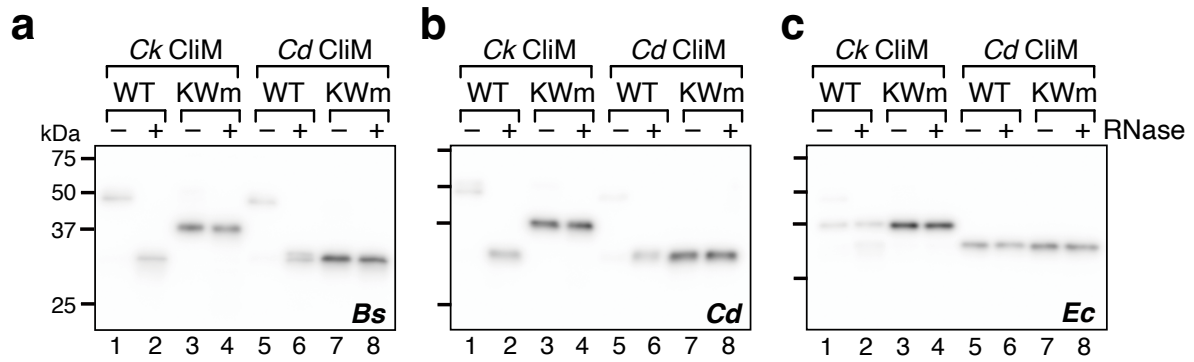
⁷ Microbiology Research Center for Sustainability (MiCS), University of Tsukuba, Tsukuba, Japan

* These authors contributed equally

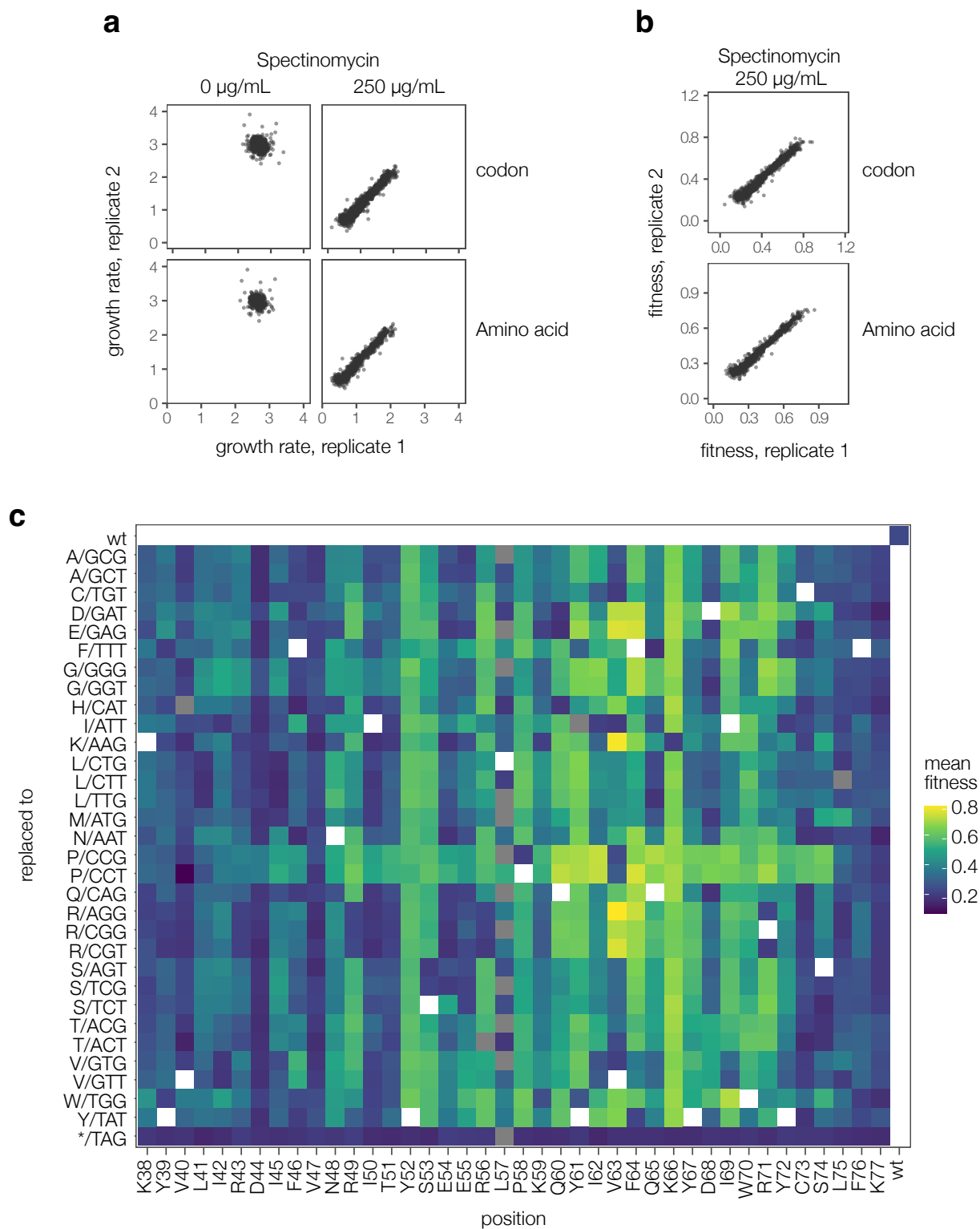
Corresponding authors:

Prof Shinobu Chiba (schiba@cc.kyoto-su.ac.jp)

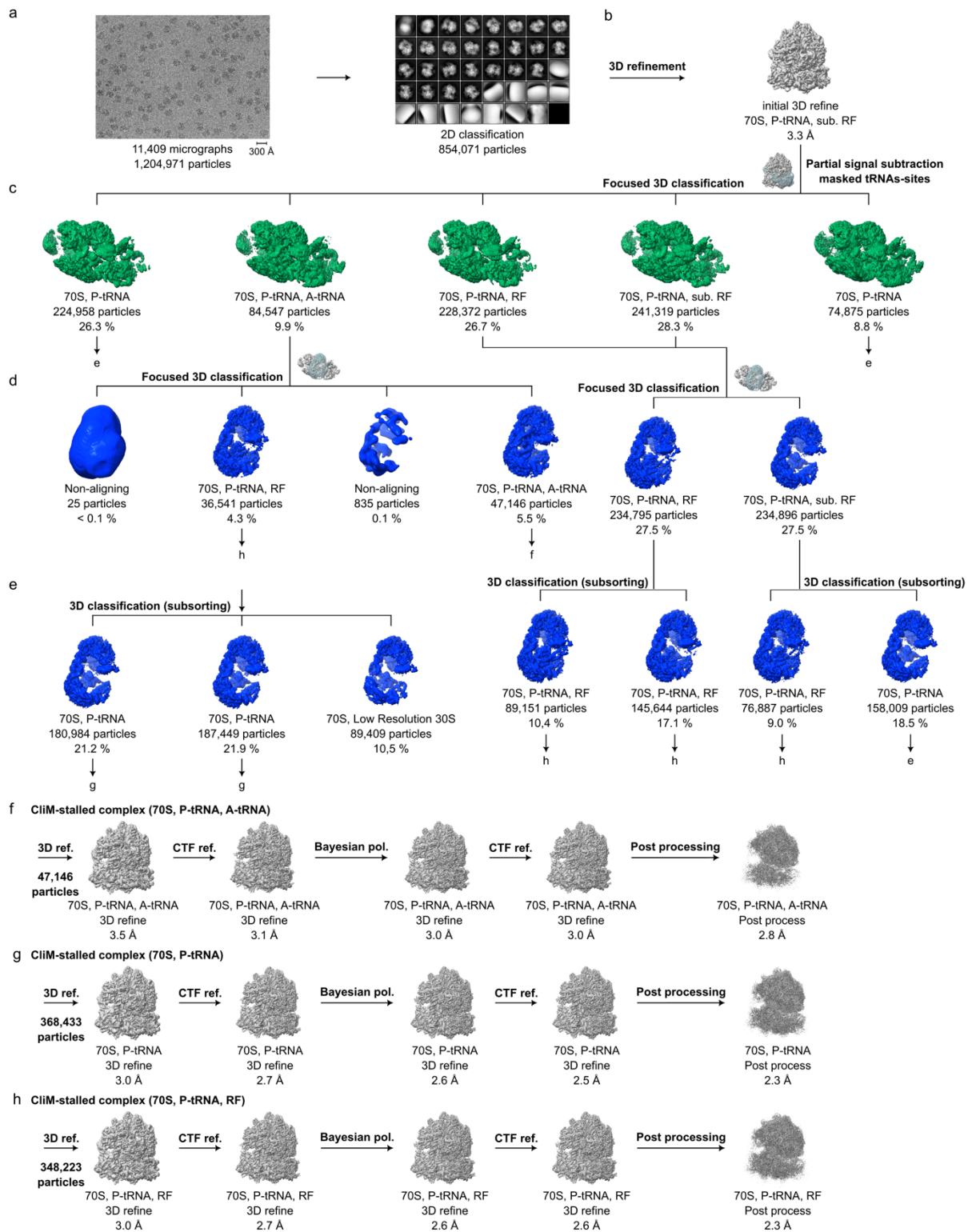
Prof Daniel N. Wilson (Daniel.wilson@uni-hamburg.de)



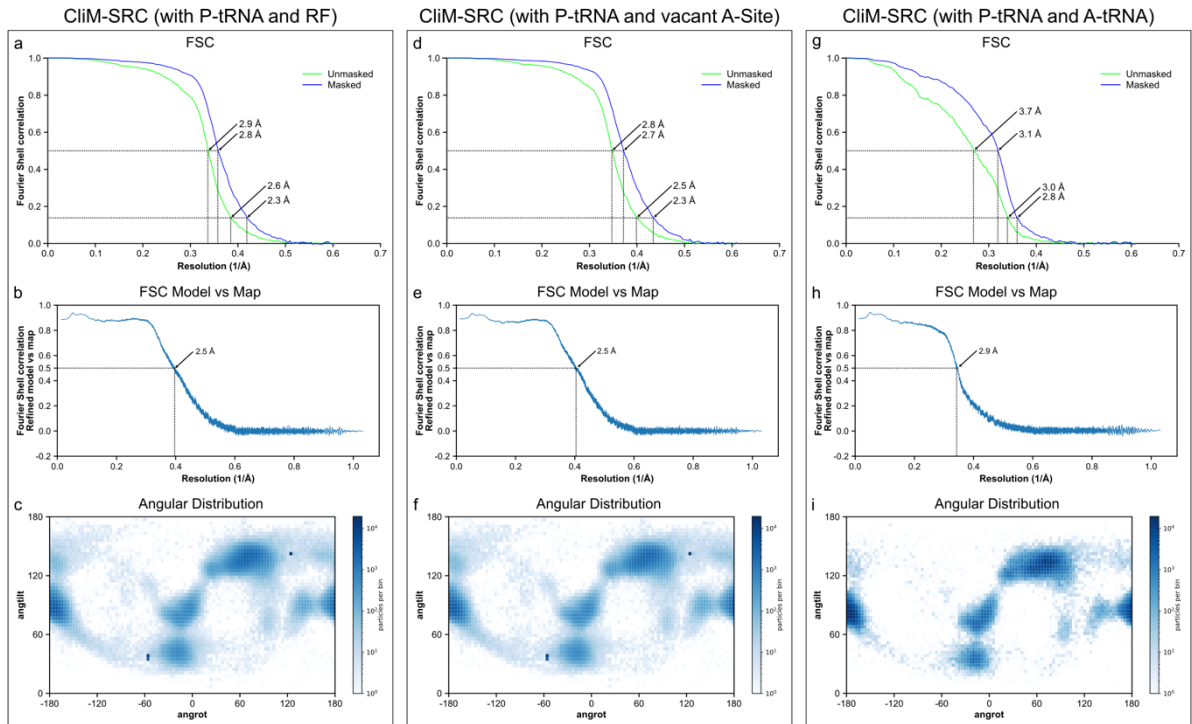
Supplementary Fig. 1: Ck and Cd CliM arrest Bs and Cd ribosomes. a-c Western blot analysis of the in vitro translation products of Ck and Cd CliM. WT or KWm mutant derivatives of the *gfp-cliM-myc-lacZ α* translational fusion reporters were translated in the Bs PURE (a), Cd PURE (b), or Ec PURE (c). The products were separated in neutral-pH gels and immunoblotted using anti-GFP antibody. Samples treated with RNase A (+) were analyzed alongside untreated samples (-) to distinguish peptidyl-tRNA from full-length hydrolyzed products. Molecular size markers (kDa) are shown on the left. Western blotting was independently repeated at least twice to ensure reproducibility. Source data are provided as a Source Data file.



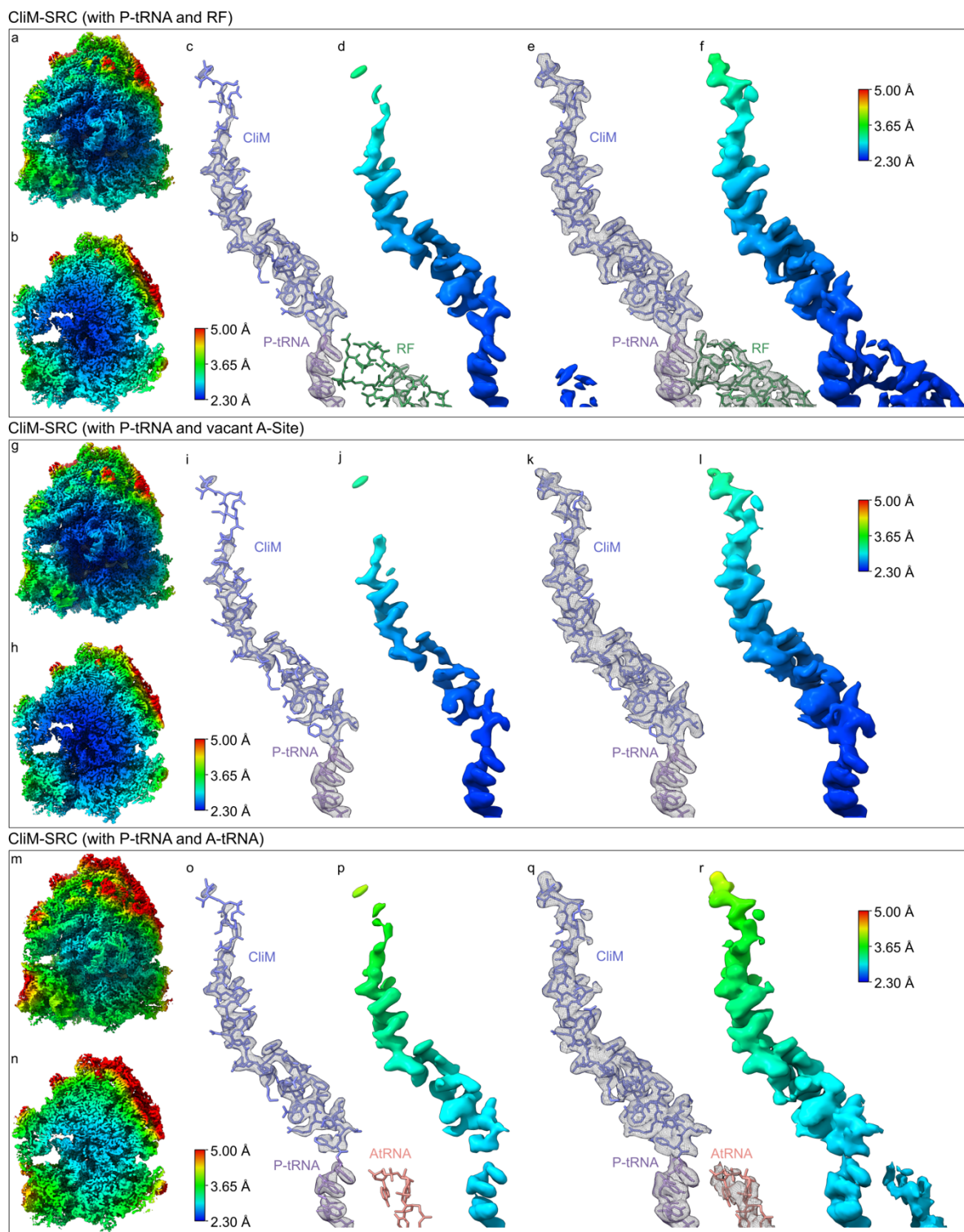
Supplementary Fig. 2: Reproducibility of Deep mutational scanning. (a-b) Scatter plots of growth rates (a) and fitness values (b) of each variant are shown at the codon level (upper) and at the amino acid level (lower), where amino acid-level values were obtained by averaging synonymous codon variants. In each plot, biological replicate 1 is shown on the x-axis and biological replicate 2 on the y-axis, demonstrating reproducibility across replicates. (c) The heatmap shows the relative fitness of each variant at the codon level, calculated as the mean of two biological replicates (related to Fig. 3), demonstrating that synonymous codon variants generally exhibit similar fitness values. Residue numbers and wild-type amino acids are indicated along the bottom, and substituted residues are shown along the left.



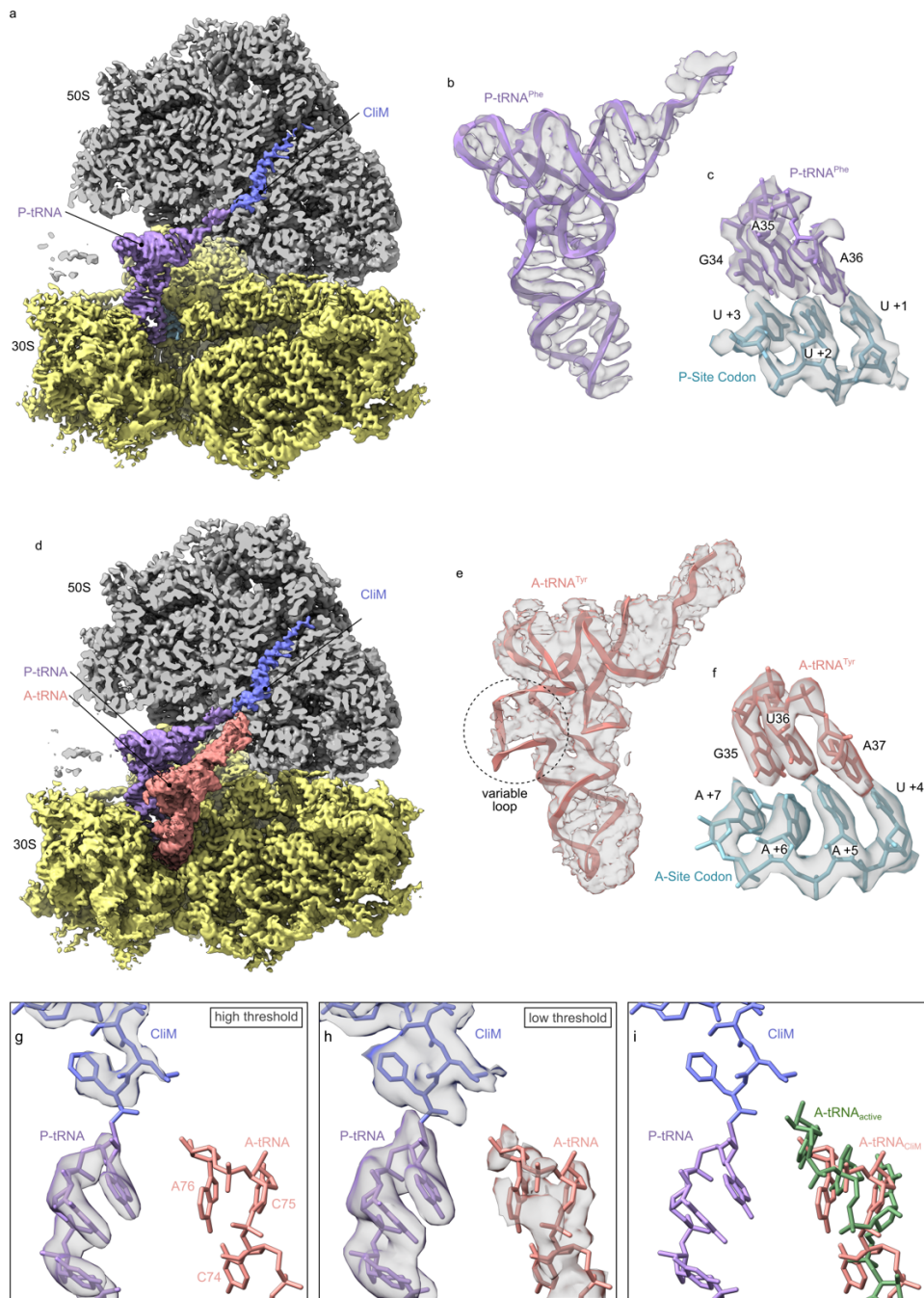
Supplementary Fig. 3: *In silico* sorting scheme for CiIM. (a) From 11,409 micrographs, 1,204,971 particles were picked and subjected to 2D classification resulting in 854,071 ribosome-like particles. Particles were (b) initially 3D-refined, then (c) subsorted into 5 classes using a mask around the tRNA binding sites. (d-e) The resulting classes with P-tRNA and vacant A-site, PtRNA and release factor as well as PtRNA and A-tRNA were further subsorted with a mask around the A-site until homogeneity was reached. The minor class with (f) both A- and P-tRNA density (5.5%) resulted in a final resolution (at FSC 0.143) of 2.8 Å. After combining of the respective particles, two major classes with (g) P-tRNA and vacant A-site (43.1%) as well as (h) P-tRNA and release factor (40.8%) resulted in a final resolution (at FSC 0.143) of 2.3 Å, respectively.



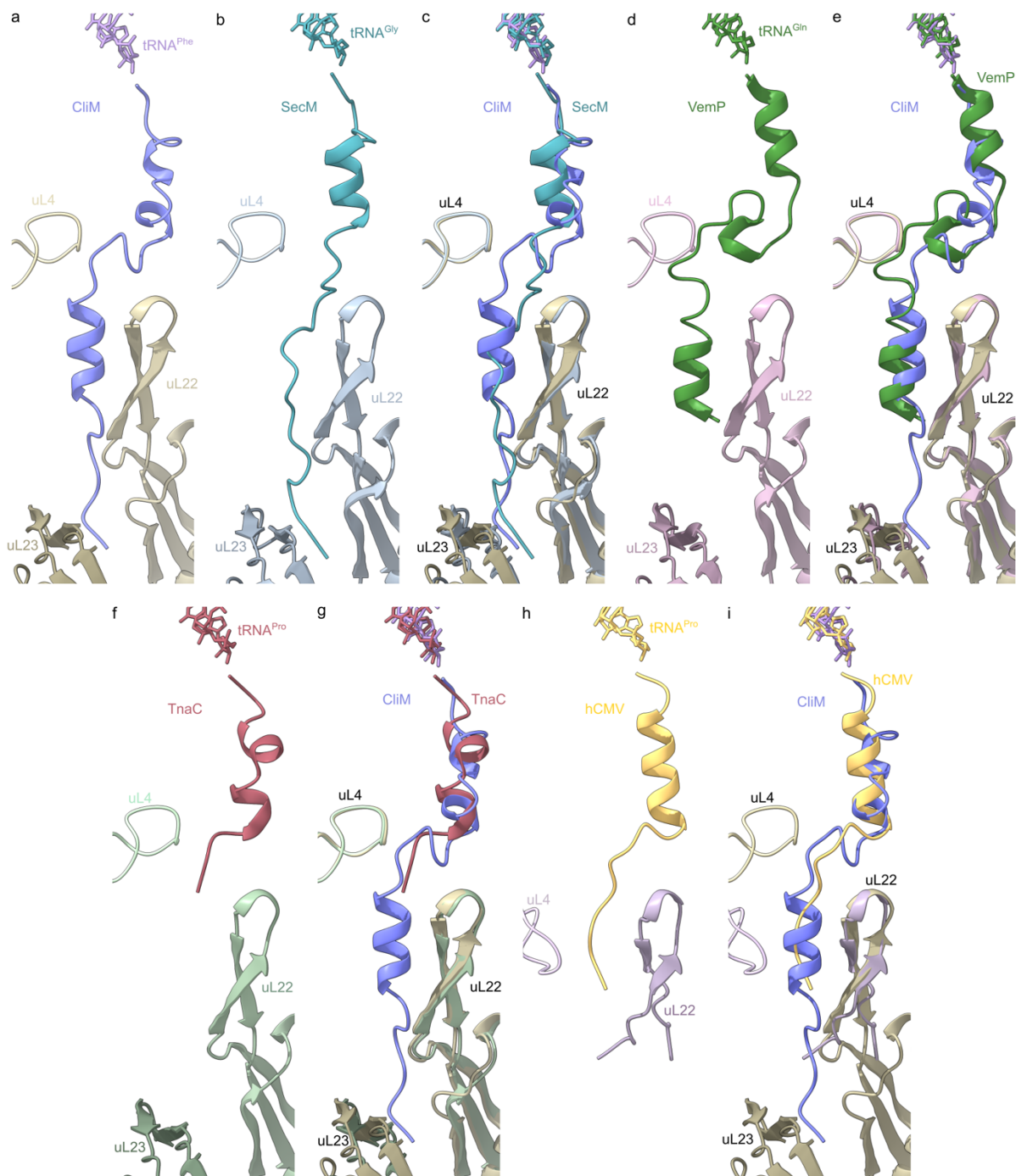
Supplementary Fig. 4: Fourier Shell Correlation curves and angular distribution for CliM-SRC. (a-c) Fourier shell correlation (FSC) curve of the (a) CliM-SRC containing P-tRNA and RF, (b) with P-tRNA and vacant A-site and (c) with P-tRNA and A-tRNA, with unmasked (green) and masked (blue) FSC curves plotted against the resolution ($1/\text{\AA}$). (d-f) Refined model vs map FSC curve of the CliM-SRC from (a)-(c) plotted against the resolution ($1/\text{\AA}$). (g-i) Angular distribution of particles used for 3D reconstruction from Relion for the CliM-SRC from (a)-(c). Particles are binned and logarithmical represented from white to blue.



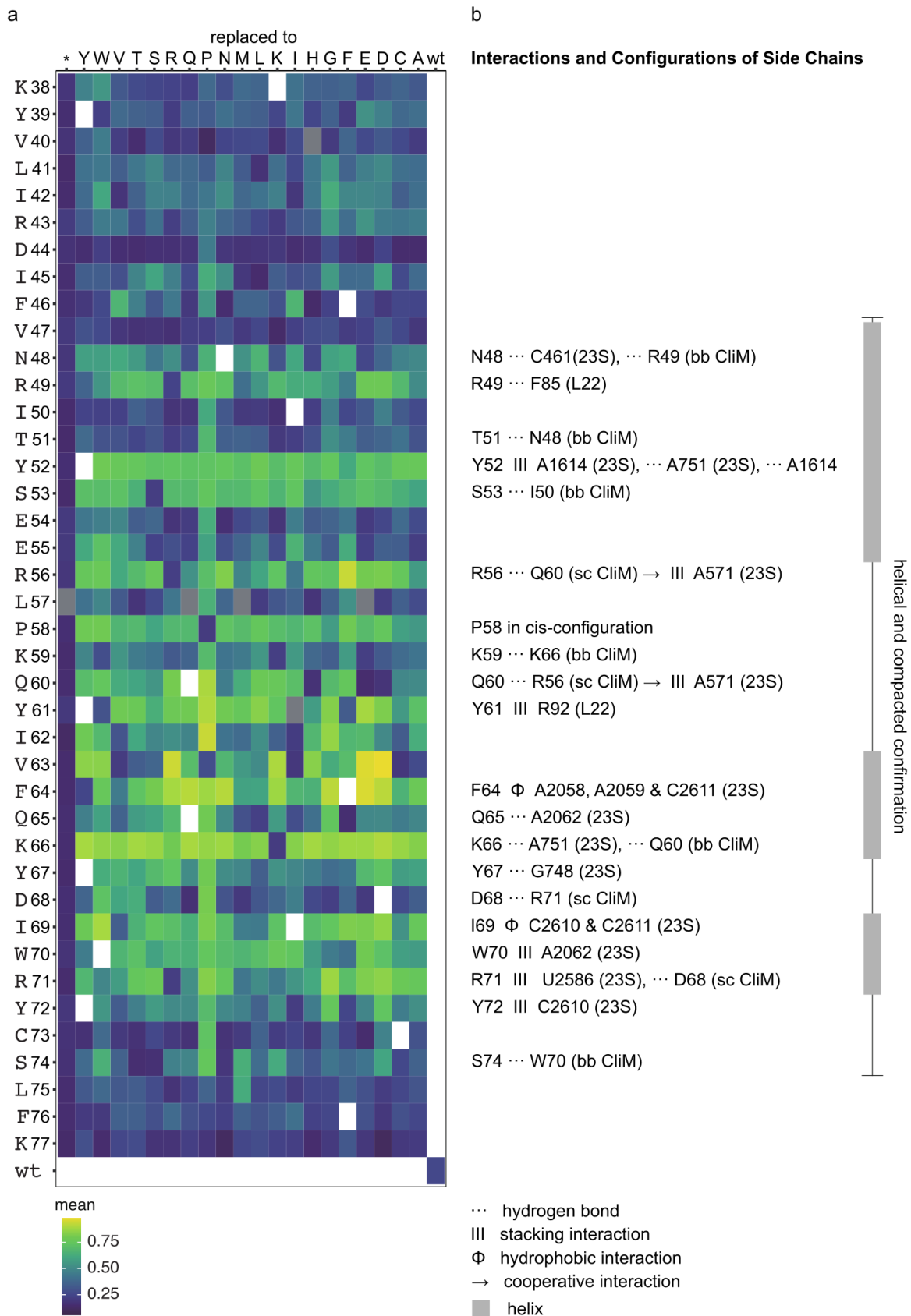
Supplementary Fig. 5: Local resolution for the CliM-SRCs. (a-r) Cryo-EM density for the 3D-refined map of the CliM-SRC with (a-f) P-tRNA and RF, (g-l) P-tRNA and vacant A-site, and (m-r) P-tRNA and A-tRNA, coloured according local resolution, or as transparent grey surface (c, e, i, k, o, q) with molecular model of the CliM-SRC taken from RF bound complex, and with A-tRNA (orange) in (o,q). In (a,g,m), overviews of the cryo-EM maps of the CliM-SRC are shown, whereas in (b,h,n), a transverse section reveals the core of the 50S subunit, including the ribosomal exit tunnel. In (e-f, k-l, q-r) the same representation is shown as in (c-d, i-j, o-p) but at a lower threshold.



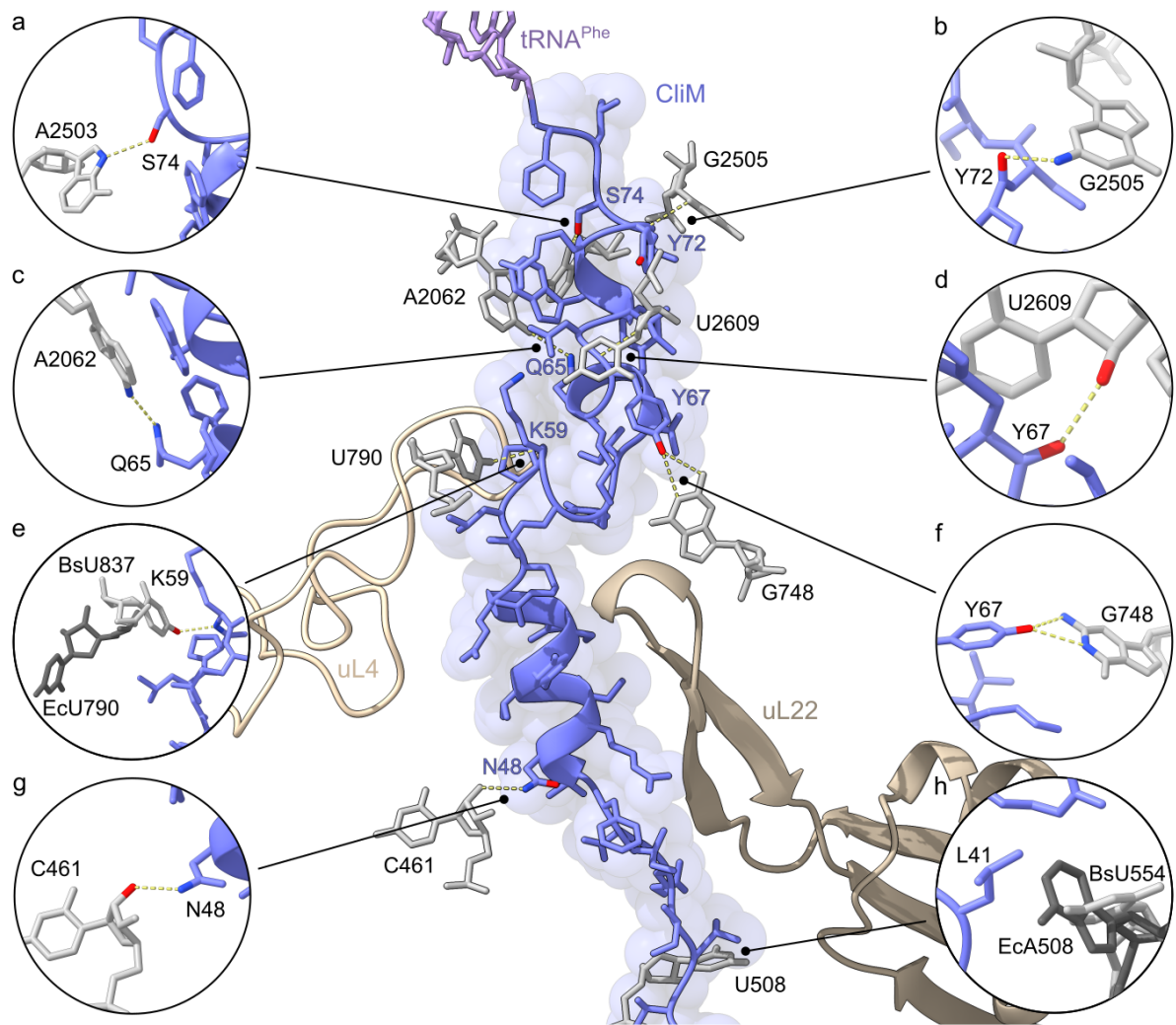
Supplementary Fig. 6: Cryo-EM density for the P-tRNA and A-tRNA. (a) Cryo-EM density for the 3D-refined map of the CliM-SRC (30S, yellow; 50S grey) with P-tRNA (purple) and vacant A-site, and transverse section of the 50S showing CliM nascent chain (blue) within the exit tunnel. (b-c) cryo-EM map density (transparent grey) for (b) the P-tRNA from (a) with fitted model for tRNA^{Phe} (purple), and (c) anticodon of tRNA^{Phe} in the P-site base-pairing with the UUU codon (positions +1 to +3) of the mRNA (green). (d) Cryo-EM density for the 3D-refined map of the CliM-SRC (30S, yellow; 50S grey) with P-tRNA (purple) and A-tRNA, and transverse section of the 50S showing CliM nascent chain (blue) within the exit tunnel. (e-f) cryo-EM map density (transparent grey) for (e) the A-tRNA from (d) with fitted model for tRNA^{Tyr} (brown), and (f) anticodon of tRNA^{Tyr} in the P-site base-pairing with the UAA stop codon (positions +4 to +6) of the mRNA (green). (g-i) View of the PTC of the (g-h) A-tRNA (rose) containing state of CliM (blue) that shows a flexible CCA-end of the A-tRNA by missing density at (g) high threshold, and (h) low threshold with noisy density, and no proper accommodation shown by the comparison with a (i) CCA-end of an properly accommodated tRNA (green) (PDB ID 8CVK)¹, in the A-site of the PTC.



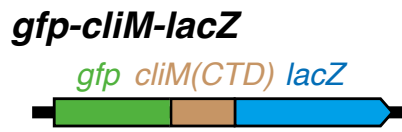
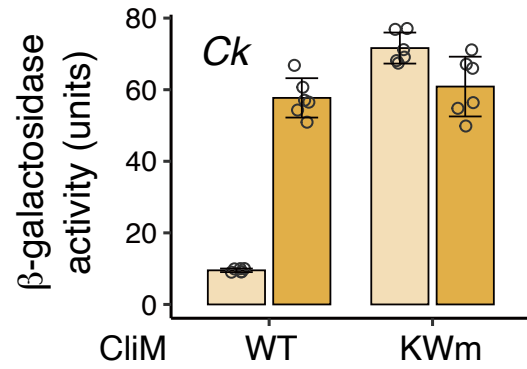
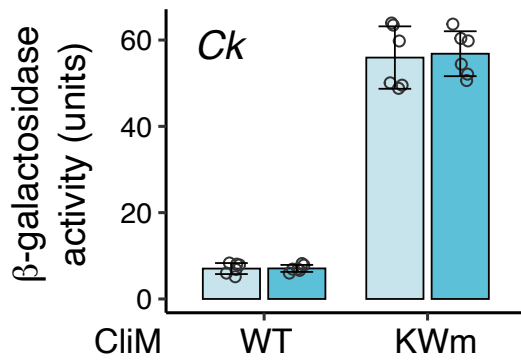
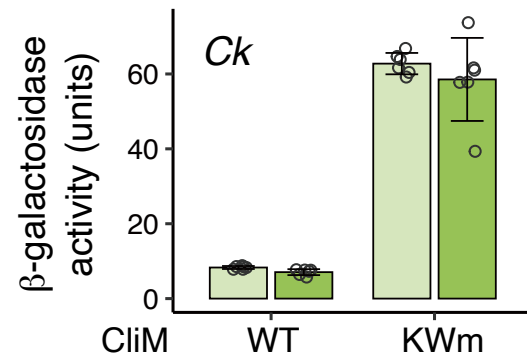
Supplementary Fig. 7: Comparison of CliM with SecM, VemP and TnaC arrest peptides. (a) CliM (blue) attached to the P-tRNA (lavender) in relation to uL4 (light gold), uL22 (gold) and uL23 (dark gold). (b) SecM (PDB ID 8QOA)² attached to the P-tRNA (teal) in relation to uL4 (light slate blue), uL22 (slate blue) and uL23 (dark slate blue). (c) Overlay (aligned on the basis of 23S rRNA) of (a) CliM and (b) SecM. (d) VemP (PDB ID 5NWX)³ attached to the P-tRNA (green) in relation to uL4 (light rose), uL22 (rose) and uL23 (dark rose). (e) Overlay (aligned on the basis of 23S rRNA) (a) CliM and (d) VemP. (f) TnaC (PDB ID 7O19)⁴ attached to the P-tRNA (red) in relation to uL4 (light mint), uL22 (mint) and uL23 (dark mint). (g) Overlay (aligned on the basis of 23S rRNA) of (a) CliM and (f) TnaC. (h) hCMV (PDB ID 5A8I)⁵ attached to the P-tRNA (gold) in relation to uL4 (pink) and uL22 (purple). (i) Overlay (aligned on the basis of 23S rRNA) of (a) CliM and (h) hCMV.



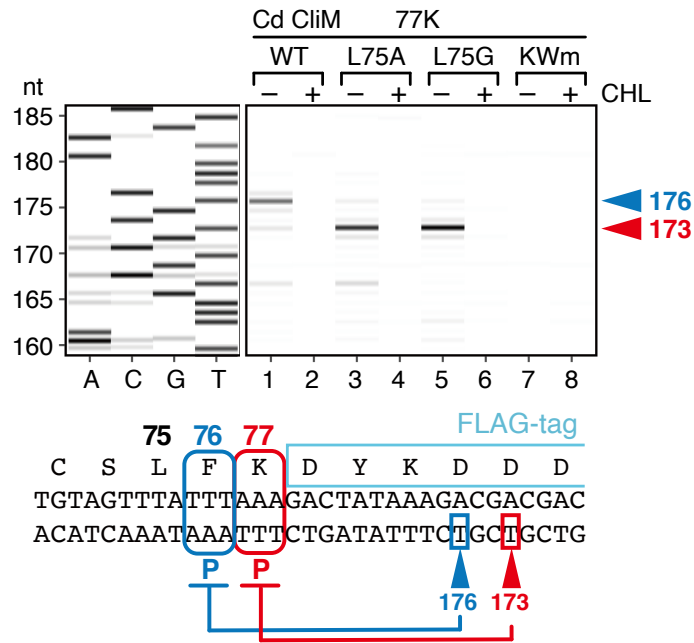
Supplementary Fig. 8: Correlation between DMS-seq and cryo-EM data for CliM. **a**, Heatmap from Fig 3c of relative fitness (mean of two biological replicate) of each CliM mutant compared with **b**, interactions of CliM sidechain observed in the cryo-EM structure of CliM-SRC. CliM secondary structure is also indicated.



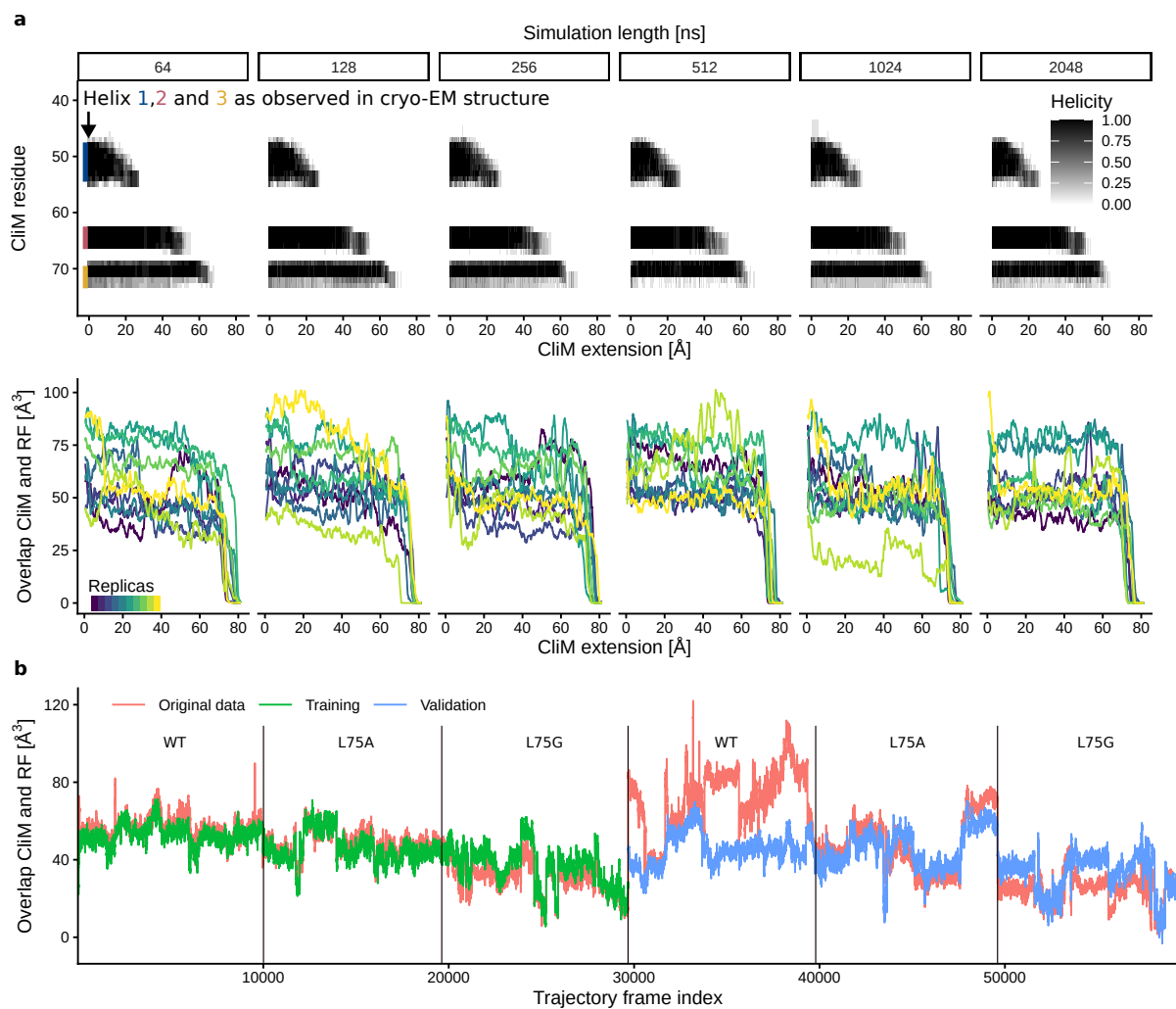
Supplementary Fig. 9: Interaction of CliM with nucleotides of the 23S rRNA. (a-h) The central panel shows the CliM nascent chain (blue) attached to the P-site tRNA (lavender) and ribosomal proteins uL4 (light gold) and uL22 (gold), with selected contacts with the 23S rRNA (grey) highlighted by individual panels. Dashed yellow lines indicated potential hydrogen bond interactions.

a**b uL22****c uL4****d uL23**

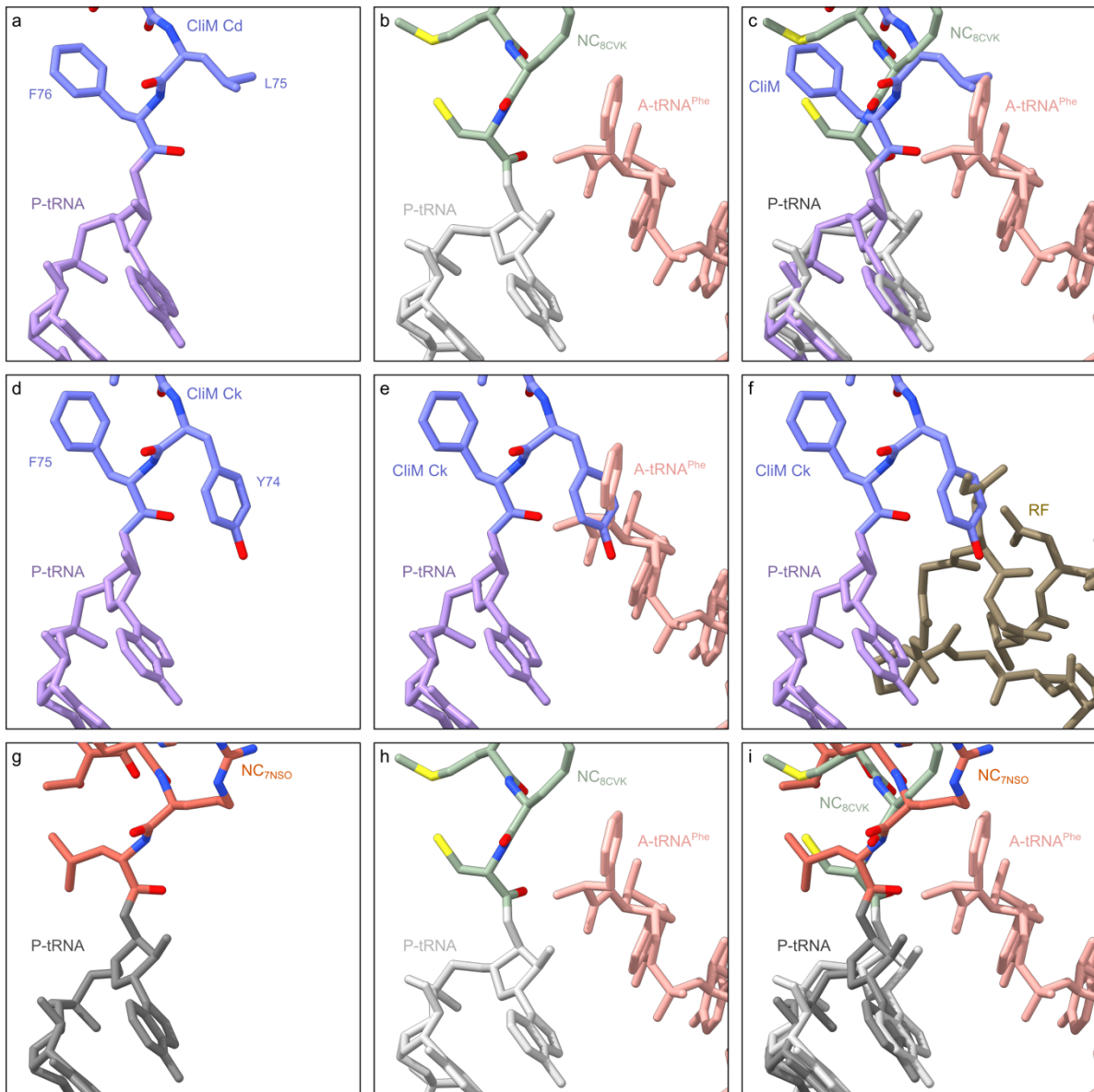
Supplementary Fig. 10: Mutation in uL22 abolishes arrest by Ck CliM. **a** Schematic representation of *gfp-cliM-lacZ* reporter. A gene fragment encoding the C-terminal domain (CTD) of Ck CliM was fused in-frame with *gfp* and *lacZ*. **b-d** β -galactosidase activity (mean \pm s.d., n=6, biologically independent cultures) of *B. subtilis* cells carrying WT or KWm derivatives of the *gfp-cliM-lacZ* reporter with (dark bars) or without (light bars) loop deletions in uL22 (b), uL4 (c), or uL23 (d). Source data are provided as a Source Data file.



Supplementary Fig. 11: Flexible stalling site selection determined by local sequence context. Toeprinting analysis of WT and Leu75 mutant derivatives of Cd CliM with substitution of the stop codon by Lys (77K). The reverse translation products were analyzed by capillary sequencer and signals were represented as a gel-style heatmap. In vitro translation was performed in the presence or absence of chloramphenicol (CHL). The toeprint length (nt) were calibrated against dideoxy sequencing (left). The estimated stalling sites (P-site codon) based on the toeprint length are shown with their codon numbers (bottom). Toeprinting analysis was independently repeated at least twice to ensure reproducibility. Source data are provided as a Source Data file.



Supplementary Fig. 12: CliM dynamics during constant-velocity pulling MD simulations and cross-validation of functional mode analysis (FMA). (a) Top panel: For different pulling simulation lengths, the time evolution of the helicity per residue is shown. Helicity is defined as the average of secondary structure states (1: Residue part of helix, 0: Residue not part of helix) over 10 independent simulation replicas. Colored bars in the leftmost panel show the secondary structure of the cryo-EM model. Bottom panel: Time evolution of the overlap volume between CliM and aligned RF for each simulation replica. (b) Comparison of measured overlap volume for frames of all unbiased MD simulation trajectories (WT and L75A, L75G mutants, red line) with overlap volume predicted from FMA (green for training, blue for validation).



Supplementary Fig. 13: Comparison of CliM with accommodated A-tRNA. (a) View of the PTC of the A-tRNA containing state of CliM (blue) attached to the P-tRNA (purple). (b) View of the PTC of a pre-attack state (PDB ID 8CVK)¹, showing a tripeptidyl-NH-tRNA (green/light grey) at the P-site and a phenyl-NH-tRNA (rose) at the A-site. (c) Overlay of (a) and (b) (aligned on the basis of 23S rRNA) highlighting the incompatibility of CliM's penultimate residue Leu75 position and an accommodated aminoacyl-tRNA moiety in the A-site of the PTC. (d) In silico created CliM Ck (blue) mutated from CliM Cd attached to the P-tRNA (purple). (e-f) Overlay of (d) CliM Ck with (e) phenyl-NH-tRNA (rose) (PDB ID 8CVK)¹ and (f) release factor 1 (brown) (PDB ID 9MTP)⁶ in the A-site, highlighting the incompatibility of proper accommodation into the A-site of the PTC for both with Tyr in the penultimate position of the CliM nascent peptide. (g) View of the PTC of stalled ErmDL peptide (red)(PDB ID 7NSO)⁷ attached to the P-tRNA (dark grey). (h) Same panel as in (b). (i) Overlay of (g) and (h) (aligned of the basis of 23S rRNA) highlighting the similarity of ErmDL- and CliM-induced stalling by encroaching penultimate nascent peptide residues into the A-site that are incompatible with proper accommodation of an aminoacyl-tRNA moiety in the A-site of the PTC.

Supplementary Table 1: Strain list

strain	plasmid	host	genotype
SCB4668	pCH2713	SCB3065	spoIIJ Ω kan, amyE::Ck_CliM-lacZ Ω cat
SCB4669	pCH2714	SCB3065	spoIIJ Ω kan, amyE::Ck_CliM(dTM)-lacZ Ω cat
SCB4670	pCH2715	SCB3065	spoIIJ Ω kan, amyE::Ck_CliM(K65A/W69A)-lacZ Ω cat
SCB4671	pCH2716	SCB3065	spoIIJ Ω kan, amyE::Ck_CliM(dTM/K65A/W69A)-lacZ Ω cat
SCB4676	pCH2713	SCB2969	AspoIIIJ::tet, amyE::Ck_CliM-lacZ Ω cat
SCB4677	pCH2714	SCB2969	AspoIIIJ::tet, amyE::Ck_CliM(dTM)-lacZ Ω cat
SCB4678	pCH2715	SCB2969	AspoIIIJ::tet, amyE::Ck_CliM(K65A/W69A)-lacZ Ω cat
SCB4679	pCH2716	SCB2969	AspoIIIJ::tet, amyE::Ck_CliM(dTM/K65A/W69A)-lacZ Ω cat
SCB4696	pCH2736	SCB3065	spoIIJ Ω kan, amyE::Ck_CliM-Dstem2-yidC2(1-6)-lacZ Ω cat
SCB4697	pCH2737	SCB3065	spoIIJ Ω kan, amyE::Ck_CliM(dTM)-Dstem2-yidC2(1-6)-lacZ Ω cat
SCB4698	pCH2738	SCB3065	spoIIJ Ω kan, amyE::Ck_CliM(K65A/W69A)-Dstem2-yidC2(1-6)-lacZ Ω cat
SCB4699	pCH2739	SCB3065	spoIIJ Ω kan, amyE::Ck_CliM(dTM/K65A/W69A)-Dstem2-yidC2(1-6)-lacZ Ω cat
SCB4700	pCH2736	SCB2969	AspoIIIJ::tet, amyE::Ck_CliM-Dstem2-yidC2(1-6)-lacZ Ω cat
SCB4701	pCH2737	SCB2969	AspoIIIJ::tet, amyE::Ck_CliM(dTM)-Dstem2-yidC2(1-6)-lacZ Ω cat
SCB4702	pCH2738	SCB2969	AspoIIIJ::tet, amyE::Ck_CliM(K65A/W69A)-Dstem2-yidC2(1-6)-lacZ Ω cat
SCB4703	pCH2739	SCB2969	AspoIIIJ::tet, amyE::Ck_CliM(dTM/K65A/W69A)-Dstem2-yidC2(1-6)-lacZ Ω cat
YSB117	pKIG1225	SCB2634	rplW(d65-69) Ω kan, amyE::PmifM-gfp-Ck_cliM-lacZ Ω cat
YSB118	pYS37	SCB2634	rplW(d65-69) Ω kan, amyE::PmifM-gfp-Ck_cliM(K65A W69A)-lacZ Ω cat
YSB119	pCH2675	SCB2613	rplW Ω kanWrplB, amyE::PmifM gfp-Cd_cliM(30-76)-R71CGG_L75TTA_77K-flag-lacZ Ω cat
YSB120	pCH2691	SCB2613	rplW Ω kanWrplB, amyE::PmifM gfp-Cd_cliM(30-76)-(K66A/W70A)-R71CGG_L75TTA_77K-flag-lacZ Ω cat
YSB121	pCH2675	SCB2942	rplD(d66-70) Ω kan, amyE::PmifM gfp-Cd_cliM(30-76)-R71CGG_L75TTA_77K-flag-lacZ Ω cat
YSB122	pCH2691	SCB2942	rplD(d66-70) Ω kan, amyE::PmifM gfp-Cd_cliM(30-76)-(K66A/W70A)-R71CGG_L75TTA_77K-flag-lacZ Ω cat
YSB123	pCH2675	SCB2634	rplW(d65-69) Ω kan, amyE::PmifM gfp-Cd_cliM(30-76)-R71CGG_L75TTA_77K-flag-lacZ Ω cat
YSB124	pCH2691	SCB2634	rplW(d65-69) Ω kan, amyE::PmifM gfp-Cd_cliM(30-76)-(K66A/W70A)-R71CGG_L75TTA_77K-flag-lacZ Ω cat
YSB125	pCH2675	SCB2656	rpsS Ω kan, amyE::PmifM gfp-Cd_cliM(30-76)-R71CGG_L75TTA_77K-flag-lacZ Ω cat
YSB126	pCH2691	SCB2656	rpsS Ω kan, amyE::PmifM gfp-Cd_cliM(30-76)-(K66A/W70A)-R71CGG_L75TTA_77K-flag-lacZ Ω cat
YSB127	pCH2675	SCB2917	rpsS Ω kanWrplV(d86-90), amyE::PmifM gfp-Cd_cliM(30-76)-R71CGG_L75TTA_77K-flag-lacZ Ω cat
YSB128	pCH2691	SCB2917	rpsS Ω kanWrplV(d86-90), amyE::PmifM gfp-Cd_cliM(30-76)-(K66A/W70A)-R71CGG_L75TTA_77K-flag-lacZ Ω cat
YSB129	pCH2675	PY79	amyE::PmifM gfp-Cd_cliM(30-76)-R71CGG_L75TTA_77K-flag-lacZ Ω cat
YSB130	pCH2691	PY79	amyE::PmifM gfp-Cd_cliM(30-76)-(K66A/W70A)-R71CGG_L75TTA_77K-flag-lacZ Ω cat
YSB41	pKIG1225	PY79	amyE::PmifM-gfp-Ck_cliM-lacZ Ω cat
YSB45	pYS37	PY79	amyE::PmifM-gfp-Ck_cliM(K65A W69A)-lacZ Ω cat
YSB65	pYS47	SCB3065	spoIIJ Ω kan, amyE::PmifM-Ck_cliM-Ck_YidC2(1-6aa)-lacZ Ω cat
YSB66	pYS50	SCB3065	spoIIJ Ω kan, amyE::PmifM-Ck_cliM(dTM)-Ck_YidC2(1-6aa)-lacZ Ω cat
YSB67	pYS49	SCB3065	spoIIJ Ω kan, amyE::PmifM-Ck_cliM(K65A W69A)-Ck_YidC2(1-6aa)-lacZ Ω cat
YSB68	pYS51	SCB3065	spoIIJ Ω kan, amyE::PmifM-Ck_cliM(dTM K65A K69A)-Ck_YidC2(1-6aa)-lacZ Ω cat
YSB69	pYS47	SCB2969	AspoIIIJ::tet, amyE::PmifM-Ck_cliM-Ck_YidC2(1-6aa)-lacZ Ω cat
YSB70	pYS50	SCB2969	AspoIIIJ::tet, amyE::PmifM-Ck_cliM(dTM)-Ck_YidC2(1-6aa)-lacZ Ω cat
YSB71	pYS49	SCB2969	AspoIIIJ::tet, amyE::PmifM-Ck_cliM(K65A W69A)-Ck_YidC2(1-6aa)-lacZ Ω cat
YSB72	pYS51	SCB2969	AspoIIIJ::tet, amyE::PmifM-Ck_cliM(dTM K65A K69A)-Ck_YidC2(1-6aa)-lacZ Ω cat
YSB81	pKIG1225	SCB2613	rplW Ω kanWrplB, amyE::PmifM-gfp-Ck_cliM-lacZ Ω cat
YSB82	pYS37	SCB2613	rplW Ω kanWrplB, amyE::PmifM-gfp-Ck_cliM(K65A W69A)-lacZ Ω cat
YSB83	pKIG1225	SCB2942	rplD(d66-70) Ω kan, amyE::PmifM-gfp-Ck_cliM-lacZ Ω cat
YSB84	pYS37	SCB2942	rplD(d66-70) Ω kan, amyE::PmifM-gfp-Ck_cliM(K65A W69A)-lacZ Ω cat
YSB85	pKIG1225	SCB2656	rpsS Ω kan, amyE::PmifM-gfp-Ck_cliM-lacZ Ω cat
YSB86	pYS37	SCB2656	rpsS Ω kan, amyE::PmifM-gfp-Ck_cliM(K65A W69A)-lacZ Ω cat
YSB87	pKIG1225	SCB2917	rpsS Ω kanWrplV(d86-90), amyE::PmifM-gfp-Ck_cliM-lacZ Ω cat
YSB88	pYS37	SCB2917	rpsS Ω kanWrplV(d86-90), amyE::PmifM-gfp-Ck_cliM(K65A W69A)-lacZ Ω cat

Supplementary Table 2. Plasmid construction

plasmid	primer fw1	primer rv1	template 1	primer fw2	primer rv2	template 2	primer fw3	primer rv3	template 3	ref
pCH2126										Sakiyama 2021
pCH2527	amyE-front-1w	pDG 1662-DspcR-fw	psK69	pDG 1662-DspcR-rv	FLAG_2-7-rv	psK69	FLAG-SpcR-fw	amyE-SpcR-rv	psK69	
pCH2612	flag-fw	gfp238-rv	pCH2627	gfp238-fw	Cdf1_KYX1W-K-flag-rv	pKIG1283				
pCH2674	CIM-R71CGG-L75TTA-FLAG-1w		pCH2612							
pCH2675	flag-fw	gfp238-rv	pCH2126	gfp238-fw	flag_2-7-rv	pCH2674				
pCH2691	Cd_CIM-repro-KWm-fw	Cd_CIM-KWm-rv	pCH2675							
pCH2713	CIM-LacZ nontGA fw	Ck non TGA LacZ rv	pYS48							
pCH2714	CIM-LacZ nontGA fw	Ck non TGA LacZ rv	pYS49							
pCH2715	CIM-LacZ nontGA fw	Ck non TGA LacZ rv	pYS50							
pCH2716	CIM-LacZ nontGA fw	Ck non TGA LacZ rv	pYS51							
pCH2730	Cd_CIM-RE-77STP-FL-fw	Cd_CIM_RE-S74-rv	pCH2675							
pCH2731	Cd_CIM-RE-L75A-77STP-FL-fw	Cd_CIM_RE-S74-rv	pCH2675							
pCH2732	Cd_CIM-RE-L75G-77STP-FL-fw	Cd_CIM_RE-S74-rv	pCH2675							
pCH2736	Ck_CIM-Dstem2-fw	Ck_CIM-Dstem2-rv	pCH2717							
pCH2737	Ck_CIM-Dstem2-fw	Ck_CIM-Dstem2-rv	pCH2718							
pCH2738	Ck_CIM-Dstem2-fw	Ck_CIM-Dstem2-rv	pCH2719							
pCH2739	Ck_CIM-Dstem2-fw	Ck_CIM-Dstem2-rv	pCH2720							
pCH2764	Cd_CIM-RE-76stp-FL-fw	Cd_CIM-C73-rv	pCH2730							
pCH2765	Cd_CIM-S74L-76stp-FL-fw	Cd_CIM-C73-rv	pCH2730							
pCH2767	Cd_CIM-S74G-76stp-FL-fw	Cd_CIM-C73-rv	pCH2730							
pCH2768	Cd_CIM-S74V-76stp-FL-fw	Cd_CIM-C73-rv	pCH2730							
pCH2774	Cd_CIM-RE-L75DKK-77STP-FL-fw	Cd_CIM_RE-S74-rv	pCH2730							
pCH2779	Cd_CIM-RE-L75S-77STP-FL-fw	Cd_CIM_RE-S74-rv	pCH2730							
pCH2780	Cd_CIM-RE-L75I-77STP-FL-fw	Cd_CIM_RE-S74-rv	pCH2730							
pCH2781	Cd_CIM-RE-L75V-77STP-FL-fw	Cd_CIM_RE-S74-rv	pCH2730							
pKIG 1225										
pKIG 1283	Cd_AP_wt fw	Cd_AP_wt rv	chrDNA of C. difficile 630	myc-lacZ-fw	gfp238-rv	psK69				Fujiwara 2024
pKIG 1284	Cd_AP_wt fw	Cd_AP_stp77A rv	chrDNA of C. difficile 630	myc-lacZ-rv	gfp238-rv	psK69				
pKIG 1285	Cd_AP_wt fw	Cd_AP_stp77K rv	chrDNA of C. difficile 630	myc-lacZ-fw	gfp238-rv	psK69				
pKIG 1288	amp121-128(TM62)	Cdf AP Q65 rv	pKIG 1283	Cdf AP K66A W70A fw	amp121-128(TM62) antisense	pKIG1283				
psK69										
pYS37	amp121-128(TM62)	uYrdC-Ob_klu-E64 rv	pKIG 1225	uYrdC_Ob_klu_K65A-W69A	amp121-128(TM62) antisense	pKIG1225				
pYS38	amp121-128(TM62)	Cd_AP_F76stp rv	pKIG 1283	myc24 fw	amp121-128(TM62) antisense	pKIG1283				
pYS39	amp121-128(TM62)	Cd_AP_F75stp rv	pKIG 1283	myc24 fw	amp121-128(TM62) antisense	pKIG1283				
pYS40	amp121-128(TM62)	Ck_AP_F76stp rv	pKIG 1225	myc24 fw	amp121-128(TM62) antisense	pKIG1225				
pYS41	amp121-128(TM62)	Ck_AP_F75stp rv	pKIG 1225	myc24 fw	amp121-128(TM62) antisense	pKIG1225				
pYS42	amp121-128(TM62)	Ck_AP_F74stp rv	pKIG 1225	myc24 fw	amp121-128(TM62) antisense	pKIG1225				
pYS47	C-kluyv-pCH746-fw	C-kluyv-pCH746 rv	uYrdC-Obst_kluyv (GeneArt Strings DNA Fragments)	lacZ_lba4-fw	PrinfM-16nt 27rv	pCH746				
pYS49	amp121-128(TM62)	uYrdC-Ob_klu-E64 rv	pYS47	uYrdC_Ob_klu_K65A-W69A	amp121-128(TM62) antisense	pYS47				
pYS50	amp121-128(TM62)	C. kluyv dele_TM12-21 rv	pYS47	C. kluyv dele_TM12-21 fw	amp121-128(TM62) antisense	pYS47				
pYS51	amp121-128(TM62)	uYrdC-Ob_klu-E64 rv	pYS49	uYrdC_Ob_klu_K65A-W69A	amp121-128(TM62) antisense	pYS49				

Supplementary Table 3: Primer list

Primer name	Sequence (5'-3')
amp121-128(TM62)	GCAGTGTGCCATAACCATGAGTG
amp121-128(TM62) antisense	CACTCATGGTTATGGCAGCACTGC
myc24 fw	GAACAAAACTCATCTCAGAAGAG
uYidC_Clo_klu_K65A-W69A	CCTAAAGACTATTTGGTCTATGAAGCATATAGAATAGCATGGTATTTTGTATATTTTAAA
uYidC-Clo_klu-E64 rv	TTCATAGACCAATAGTCTTTAGGATA
Cd_AP_F76stp rv	ATCCTCTTCTGAGATGAGTTTTTGTCTTACAAACTACAATACCTCCAATATC
Cd_AP_F75stp rv	ATCCTCTTCTGAGATGAGTTTTTGTCTTAACTACAATACCTCCAATATCATA
Ck_AP_F76stp rv	ATCCTCTTCTGAGATGAGTTTTTGTCTTAAAAATATACAAAAATACCACCATAT
Ck_AP_F75stp rv	ATCCTCTTCTGAGATGAGTTTTTGTCTTAAATATACAAAAATACCACCATATTCT
Ck_AP_F74stp rv	ATCCTCTTCTGAGATGAGTTTTTGTCTTATACAAAAATACCACCATATTCTATA
lacZ lle4-fw	ATTACGGATTCACCTGGCCGT
PmifM-16nt 27rv	GCTTCATTTTACTATATGTACAAGCTG
C-kluyv-pCH746-fw	TACATATAGTAAATGAAGCTATTGAATGGATGTGATGAAAAATAGATACTCTATTAATAA
C-kluyv-pCH746 rv	ACGGCCAGTGAATCCGTAATCATGGTATTTAAAAATATGTTTCATATAAATCCTCTCCTTA
C_kluyv dele_TM12-21 fw	ATGAAAAATAGATACTCTATTAATAATGCAAATCTGCTTTATGTTAGCACCATC
C_kluyv dele_TM12-21 rv	AATTTGCACTATTAAATAGAGTATCTATTTTCAT
PT7-RBSkf-GFP	TAACTTTAAAGAAGGAGGGAGATATACCAATGACAATGTTTGTGGGATC
lacZ60-TAATAA-21-rv	TGGTGCCGGAACACAGGCAAATATTAGCGCCATTCGCCATTCAGGCT
Universal primer-77-PURE	GAAATTAATACGACTCACTATAGGGAGACCACAACGCGTTCCCTCTAGAAAAATTTTGTAACTTTAAGAAGGAG
amyE-front-fw	TAGAGATCCGATCAGACCAGT
flag-fw	GACTATAAAGACGACGACGAC
CliM-R71CGG-L75TTA-FLAG-fw	ATTTGGCGGTATTGTAGTTTATTTAAAGACTATAAAGAC
Cd_CliM-repro-KWm-fw	TTTCAGGCATATGATATTGCGCGGTATTGTAGTTTATTT
CliM-LacZ nonTGA fw	ATTTTAAAAAAGAACCATTGATTACGGATTCAGT
Cd_CliM-RE-77STP-FL-fw	GATATTTGGCGGTATTGTAGTTTATTTAAAGACTATAAAGACGAC
Cd_CliM-RE-L75A-77STP-FL-fw	GATATTTGGCGGTATTGTAGTGCATTTTAAAGACTATAAAGACGAC
Cd_CliM-RE-L75G-77STP-FL-fw	GATATTTGGCGGTATTGTAGTGGATTTTAAAGACTATAAAGACGAC
Ck_CliM-Dstem2-fw	GTATTTTGTATATTTTAAATTCGTTGAACAAGTAAATTTAGGAA
Cd_CliM-RE-76stp-FL-fw	GATATTTGGCGGTATTGTAGTTTATAATAAGACTATAAAGACGAC
Cd_CliM-S74L-76stp-FL-fw	GATATTTGGCGGTATTGTCTTTTATAATAAGACTATAAAGACGAC
Cd_CliM-S74G-76stp-FL-fw	GATATTTGGCGGTATTGTGGTTTATAATAAGACTATAAAGACGAC
Cd_CliM-S74V-76stp-FL-fw	GATATTTGGCGGTATTGTGTTTATAATAAGACTATAAAGACGAC
Cd_CliM-RE-L75DKK-77STP-FL-fw	GATATTTGGCGGTATTGTAGTDKKTTTTAAAGACTATAAAGACGAC
Cd_CliM-RE-L75S-77STP-FL-fw	GATATTTGGCGGTATTGTAGTTCATTTTAAAGACTATAAAGACGAC
Cd_CliM-RE-L75I-77STP-FL-fw	GATATTTGGCGGTATTGTAGTATATTTTAAAGACTATAAAGACGAC
Cd_CliM-RE-L75V-77STP-FL-fw	GATATTTGGCGGTATTGTAGTGTATTTTAAAGACTATAAAGACGAC
pDG1662-DspcR-fw	AATCAACGAGGTGAAATCGCTAATTTTATTGCAATAACA
gfp238-rv	TTTGTATAGTTCATCCATGCC
CliM-R71CGG-rv	ACTACAATACCGCCAAATATCATATTTCTGAAAAACTATATACTG
Cd_CliM-KWm-rv	CGCAATATCATATGCCGAAAAACTATATACTGTTAGG
Ck non TGA LacZ rv	CCGTAATCATGGTCTTATTTTAAAAATATACAAAAATACCA
Cd_CliM_RE-S74-rv	ACTACAATACCGCCAAATATCATATTT
Ck_CliM-Dstem2-rv	ATTTTAAAAATATACAAAAATACCA
Cd_CliM-C73-rv	ACAATACCGCCAAATATCATATTTCTG
pDG1662-DspcR-rv	TATTGCAATAAAATAGCGATTTTCACCTCGTTGATTATG
gfp238-fw	GGCATGGATGAACTATACAAA
FLAG_2-7-rv	TTTGTCTGCTCGTCTTTATA
Cdif_KYxIW-K-flag-rv	GTCGTCGCTTTATAGTCTTTTAAACAAACTACAATACCTCCAAT
FLAG-SpcR-fw	TATAAAGACGACGACGACAAAAGCAATTTAATTAACGGAAAA
amyE-SpcR-rv	ACTGGTCTGATCGGATCTCTACTAATTTAGAGAAAGTTTCTAT
Cd_AP_wt fw	GGCATGGATGAACTATACAAAAAAGACCTCTTAAATCATAAAAATTAAGTATGTT
Cd_AP_wt rv	ATCCTCTTCTGAGATGAGTTTTTGTCTTAAACAAACTACAATACCTCCAATATC
Cd_AP_stp77A rv	ATCCTCTTCTGAGATGAGTTTTTGTCTGCAACAAACTACAATACCTCCAAT
Cd_AP_stp77K rv	ATCCTCTTCTGAGATGAGTTTTTGTCTTAAACAAACTACAATACCTCCAATATC
Cdif AP Q65 rv	CTGAAAAACTATATACTGTTTAGGCAG
Cdif AP K66A W70A fw	CTGCCTAAACAGTATATAGTTTTTCAGGCATATGATATTGCGAGGTATTGTAGTTTGTAAAGAA

Supplementary Table 4: Degenerate primers for DMS

Primer name	Sequence (5'-3')
Cdif_KYx1w_K77-NNK-fw2nd	TGGCGGTATTGTAGTTTATTNNKGACTIONATAAAGACGAC
Cdif_KYx1w_F76-NNK-fw2nd	ATTTGGCGGTATTGTAGTTTANNKAAAGACTATAAAGAC
Cdif_KYx1w_L75-NNK-fw2nd	GATATTTGGCGGTATTGTAGTNNKTTAAAGACTATAAA
Cdif_KYx1w_S74-NNK-fw2nd	TATGATATTTGGCGGTATTGTNNKTTATTAAAGACTAT
Cdif_KYx1w_C73-NNK-fw2nd	AAATATGATATTTGGCGGTATNNKAGTTTATTAAAGAC
Cdif_KYx1w_Y72-NNK-fw2nd	CAGAAATATGATATTTGGCGGNKGTAGTTTATTAAAA
Cdif_KYx1w_R71-NNK-fw2nd	TTTCAGAAATATGATATTTGGNNKATTGTAGTTTATT
Cdif_KYx1w_W70-NNK-fw2nd	GTTTTTCAGAAATATGATATTTNNKCGGTATTGTAGTTTA
Cdif_KYx1w_I69-NNK-fw2nd	ATAGTTTTTCAGAAATATGATNNKTTGGCGGTATTGTAGT
Cdif_KYx1w_D68-NNK-fw2nd	TATATAGTTTTTCAGAAATATNNKATTGGCGGTATTGT
Cdif_KYx1w_Y67-NNK-fw2nd	CAGTATATAGTTTTTCAGAAANNKATATTTGGCGGTAT
Cdif_KYx1w_K66-NNK-fw2nd	AAACAGTATAGTTTTTCAGNNKATGATATTTGGCGG
Cdif_KYx1w_Q65-NNK-fw	CCTAACAGTATATAGTTTTNNKAAATATGATATTTGG
Cdif_KYx1w_F64-NNK-fw	CTGCCTAACAGTATATAGTTNNKAGAAATATGATAT
Cdif_KYx1w_V63-NNK-fw	CGACTGCCTAACAGTATATANNKTTTCAGAAATATGAT
Cdif_KYx1w_I62-NNK-fw	GAACGACTGCCTAACAGTATNNKGTTTTTTCAGAAATAT
Cdif_KYx1w_Y61-NNK-fw	GAAGAAGACTGCCTAACAGNNKATAGTTTTTCAGAAA
Cdif_KYx1w_Q60-NNK-fw	TCTGAAGAAGACTGCCTAAANNKATATAGTTTTTCAG
Cdif_KYx1w_K59-NNK-fw	TATTTCTGAAGAAGACTGCCTNNKAGTATATAGTTTTT
Cdif_KYx1w_P58-NNK-fw	ACATATTTCTGAAGAAGACTGNNKAAACAGTATATAGTT
Cdif_KYx1w_L57-NNK-fw	ATTACATATTTCTGAAGAAGANNKCTAACAGTATATA
Cdif_KYx1w_R56-NNK-fw	AGAATTACATATTTCTGAAGAANNKCTGCCTAACAGTAT
Cdif_KYx1w_E55-NNK-fw	AATAGAATTACATATTTCTGAANNKCGACTGCCTAACAG
Cdif_KYx1w_E54-NNK-fw	GTAAATAGAATTACATATTTCTNNKGAACGACTGCCTAAA
Cdif_KYx1w_S53-NNK-fw	TTTTGTAATAGAATTACATATNNKGAAGAAGACTGCCT
Cdif_KYx1w_Y52-NNK-fw	ATATTTGTAAATAGAATTACANNKCTGAAGAAGACTG
Cdif_KYx1w_T51-NNK-fw	GACATATTTGTAAATAGAATTNNKATTTCTGAAGAAGCA
Cdif_KYx1w_I50-NNK-fw	AGAGACATATTTGTAAATAGANNKACATATTTCTGAAGAA
Cdif_KYx1w_R49-NNK-fw	ATAAGAGACATATTTGTAAATNNKATACATATTTCTGAA
Cdif_KYx1w_N48-NNK-fw	TTAATAAGAGACATATTTGTANNKAGAATTACATATTTCT
Cdif_KYx1w_V47-NNK-fw	GTTTTAATAAGAGACATATTTNNKAAATAGAATTACATAT
Cdif_KYx1w_F46-NNK-fw	TATGTTTTAATAAGAGACATANNKGTAAATAGAATTACA
Cdif_KYx1w_I45-NNK-fw	AAGTATGTTTTAATAAGAGACNNKTTTGTAAATAGAATT
Cdif_KYx1w_D44-NNK-fw	ATTAAGTATGTTTTAATAAGANNKATATTTGTAAATAGA
Cdif_KYx1w_R43-NNK-fw	AAAATTAAGTATGTTTTAATANNKAGACATATTTGTAAAT
Cdif_KYx1w_V42-NNK-fw	CATAAAATTAAGTATGTTTTANNKAGAGACATATTTGTA
Cdif_KYx1w_L41-NNK-fw	AATCATAAAATTAAGTATGTTNNKATAAGAGACATATTT
Cdif_KYx1w_V40-NNK-fw	TTAAATCATAAAATTAAGTATNNKTTAAATAGAGACATA
Cdif_KYx1w_Y39-NNK-fw	CTCTTAAATCATAAAATTAAGNNKGTTTTTAATAAGAGAC
Cdif_KYx1w_K38-NNK-fw	GACCTCTTAAATCATAAAATNNKATGTTTTAATAAGA
Cdif_KYx1w_L75-rv2nd	TAAACTACAATACCGCCAAATATCATA
Cdif_KYx1w_C73-rv2nd	ACAATACCGCCAAATATCATAATTTCTG
Cdif_KYx1w_R71-rv2nd	CCGCCAAATATCATAATTTCTGAAAAAC
Cdif_KYx1w_I69-rv	AATATCATAATTTCTGAAAAACTATATA
Cdif_KYx1w_Y67-rv	TTTCTGAAAAACTATATACTGTTTAGG
Cdif_KYx1w_Q65-rv	CTGAAAAACTATATACTGTTTAGGCAG
Cdif_KYx1w_V63-rv	TATATACTGTTTAGGCAGTCGTTCTTC
Cdif_KYx1w_Y61-rv	CTGTTTAGGCAGTCGTTCTTCAGAATA
Cdif_KYx1w_K59-rv	AGGCAGTCGTTCTTCAGAATATGTAAT
Cdif_KYx1w_L57-rv	TCGTTCTTCAGAATATGTAATTTCTATT
Cdif_KYx1w_E55-rv	TTCAGAATATGTAATTTCTATTACAAA
Cdif_KYx1w_S53-rv	ATATGTAATTTCTATTACAAATATGTC
Cdif_KYx1w_T51-rv	AATTTCTATTACAAATATGTTCTTTAT
Cdif_KYx1w_R49-rv	ATTTACAAATATGTTCTTTATTAAC
Cdif_KYx1w_V47-rv	AAATATGTTCTTTATTAACATACTT
Cdif_KYx1w_I45-rv	GTTCTTTATTAACATACTTTAATTTATG
Cdif_KYx1w_R43-rv	TCTTTATTAACATACTTTAATTTATG
Cdif_KYx1w_L41-rv	AACATACTTAATTTATGATTTAAGAG
Cdif_KYx1w_Y39-rv	CTTAATTTATGATTTAAGAGGTTCTTT
Cdif_KYx1w_I37-rv	AATTTATGATTTAAGAGGTTCTTTTT

Supplementary Table 5: Primers used for preparation of NGS library

Primer name	Sequence(5'-3')
P5-UDI0001-Rd1-TAG-gfp215-fw	AATGATACGGCGACCACCGAGATCTACACAGCGCTAGACACTCTTCCCTACACGACGCTC TTCCGATCTNNNNNNTAGAGAGACCACATGGTCCTTCTT
P7-UDI0001-Rd2-ACC-FLAG2-8-rv	CAAGCAGAAGACGGCATAACGAGATAACCGCGGGTGACTGGAGTTCAGACGTGTGCTCTTC CGATCTNNNNNNACCTTTGTCGTCGTCGTCCTTTATA
P7-UDI0001-Rd2-AGC-FLAG2-8-rv	CAAGCAGAAGACGGCATAACGAGATAACCGCGGGTGACTGGAGTTCAGACGTGTGCTCTTC CGATCTNNNNNNAGCTTTGTCGTCGTCGTCCTTTATA
P7-UDI0001-Rd2-AGG-FLAG2-8-rv	CAAGCAGAAGACGGCATAACGAGATAACCGCGGGTGACTGGAGTTCAGACGTGTGCTCTTC CGATCTNNNNNNAGGTTTGTGTCGTCGTCGTCCTTTATA
P7-UDI0001-Rd2-CTC-FLAG2-8-rv	CAAGCAGAAGACGGCATAACGAGATAACCGCGGGTGACTGGAGTTCAGACGTGTGCTCTTC CGATCTNNNNNNCTCTTTGTGTCGTCGTCGTCCTTTATA
P7-UDI0001-Rd2-CTG-FLAG2-8-rv	CAAGCAGAAGACGGCATAACGAGATAACCGCGGGTGACTGGAGTTCAGACGTGTGCTCTTC CGATCTNNNNNNCTGTTTGTGTCGTCGTCGTCCTTTATA
P7-UDI0001-Rd2-TGC-FLAG2-8-rv	CAAGCAGAAGACGGCATAACGAGATAACCGCGGGTGACTGGAGTTCAGACGTGTGCTCTTC CGATCTNNNNNNTGCTTTGTGTCGTCGTCGTCCTTTATA
P7-UDI0001-Rd2-TTA-FLAG2-8-rv	CAAGCAGAAGACGGCATAACGAGATAACCGCGGGTGACTGGAGTTCAGACGTGTGCTCTTC CGATCTNNNNNNTTATTTGTGTCGTCGTCGTCCTTTATA
P7-UDI0001-Rd2-TTG-FLAG2-8-rv	CAAGCAGAAGACGGCATAACGAGATAACCGCGGGTGACTGGAGTTCAGACGTGTGCTCTTC CGATCTNNNNNNTTGTTTGTGTCGTCGTCGTCCTTTATA

Supplementary Table 6: MD simulation checklist.

Reliability and reproducibility checklist for molecular dynamics simulations *All boxes must be marked YES by acceptance unless an N/A option is available	Yes	N/A	Response (Please state where this information can be found in the text)
1. Convergence of simulations and analysis			
1a. Is an evaluation presented in the text to show that the property being measured has equilibrated in the simulations (<i>e.g.</i> time-course analysis)?	<input checked="" type="checkbox"/>		See ED Fig. 7b
1b. Then, is it described in the text how simulations are split into equilibration and production runs and how much data were analyzed from production runs?	<input checked="" type="checkbox"/>		See Methods: MD simulation Set-up
1c. Are there at least 3 simulations per simulation condition with statistical analysis?	<input checked="" type="checkbox"/>		10 replica simulations per condition each. See Methods: MD simulation setup.
1d. Is evidence provided in the text that the simulation results presented are independent of initial configuration?	<input checked="" type="checkbox"/>		Evidence is provided in Figure 8a, showing that a wide conformational space around the cryo-EM model is explored by CliM NC.
2. Connection to experiments			
2a. Are calculations provided that can connect to experiments (<i>e.g.</i> loss or gain in function from mutagenesis, binding assays, NMR chemical shifts, J-couplings, SAXS curves, interaction distances or FRET distances, structure factors, diffusion coefficients, bulk modulus and other mechanical properties, <i>etc.</i>)?	<input checked="" type="checkbox"/>		Mutagenesis experiments of stalling critical residue L75 (Fig. 7) were complemented and compared with MD simulations (Fig. 8a).
3. Method choice			
3a. Is it described in the text what force field and water model are used and why?	<input checked="" type="checkbox"/>		See Methods: MD simulation Set-up
3b. Do simulations contain membranes, membrane proteins, intrinsically disordered proteins, glycans, nucleic acids, polymers, or cryptic ligand binding?	<input checked="" type="checkbox"/>	<input type="checkbox"/>	Nucleic acids

	If 3b is YES , are enhanced sampling methods used?	<input type="checkbox"/>	<input checked="" type="checkbox"/>	Response not needed if N/A
	If enhanced sampling methods are used, are the convergence criteria clearly stated?	<input type="checkbox"/>		
	If 3b is YES , is it explained in the text why or why not enhanced sampling methods are used?	<input type="checkbox"/>		
4. Code and reproducibility				
	4a. Is a table provided describing the system setup, such as simulation box dimensions, total number of atoms, total number of water molecules, salt concentration, lipid composition (number of molecules and type)?	<input checked="" type="checkbox"/>		See Methods: MD simulation setup.
	4b. Is it described in the text what simulation and analysis software and which versions are used?	<input checked="" type="checkbox"/>		See Methods: MD simulation setup.
	4c. Are initial coordinate and simulation input files and a coordinate file of the final output provided as supplementary files or in a public repository?	<input checked="" type="checkbox"/>		https://doi.org/10.5281/zenodo.17779011
	4d. Is there custom code or custom force field parameters?	<input type="checkbox"/>	<input checked="" type="checkbox"/>	Response not needed if N/A
	If YES , are they provided as supplementary profiles or in a public repository?	<input type="checkbox"/>		

Supplementary References

1. Syroegin, E. A., Aleksandrova, E. V & Polikanov, Y. S. Insights into the ribosome function from the structures of non-arrested ribosome-nascent chain complexes. *Nat. Chem.* 15, 143–153 (2023).
2. Gersteuer, F. *et al.* The SecM arrest peptide traps a pre-peptide bond formation state of the ribosome. *Nat. Commun.* 15, 2431 (2024).
3. Su, T. *et al.* The force-sensing peptide VemP employs extreme compaction and secondary structure formation to induce ribosomal stalling. *Elife* 6, (2017).
4. van der Stel, A.-X. *et al.* Structural basis for the tryptophan sensitivity of TnaC-mediated ribosome stalling. *Nat. Commun.* 12, 5340 (2021).
5. Matheisl, S., Berninghausen, O., Becker, T. & Beckmann, R. Structure of a human translation termination complex. *Nucleic Acids Res.* 43, 8615–26 (2015).
6. Aleksandrova, E. V *et al.* Mechanism of release factor-mediated peptidyl-tRNA hydrolysis on the ribosome. *Science* 388, eads9030 (2025).
7. Beckert, B. *et al.* Structural and mechanistic basis for translation inhibition by macrolide and ketolide antibiotics. *Nat. Commun.* 12, 4466 (2021).